Transverse negative magnetoresistance of two-dimensional structures in the presence of a strong in-plane magnetic field: Weak localization as a probe of interface roughness

G. M. Minkov,* O. E. Rut, A. V. Germanenko, and A. A. Sherstobitov
Institute of Physics and Applied Mathematics, Ural State University, 620083 Ekaterinburg, Russia

B. N. Zvonkov
Physical-Technical Research Institute, University of Nizhni Novgorod, Nizhni Novgorod 603600, Russia

V. I. Shashkin and O. I. Khrykin
Institute of Physics of Microstructures of RSA, 603600 Nizhni Novgorod, Russia

D. O. Filatov
Research and Educational Center for Physics of the Solid State Nanostructures, University of Nizhni Novgorod, Nizhni Novgorod 603600, Russia

(Received 14 November 2003; revised manuscript received 11 March 2004; published 13 July 2004)

The interference induced transverse negative magnetoresistance of $GaAs/In_xGa_{1-x}As/GaAs$ quantum well heterostructures has been studied in the presence of strong in-plane magnetic field. It is shown that the effect of in-plane magnetic field is determined by the interface roughness and strongly depends on the relationship between mean free path, phase breaking length, and roughness correlation length. Analysis of the experimental results allows us to estimate parameters of short- and long-range correlated roughness which have been found in a good agreement with atomic force microscopy data obtained for just the same samples.

DOI: 10.1103/PhysRevB.70.035304 PACS number(s): 73.20.Fz, 73.61.Ey

I. INTRODUCTION

The interference correction determines in the main the temperature and magnetic field dependences of the conductivity of weakly disordered two-dimensional (2D) systems. This correction originates in the constructive interference of time-reversed electron trajectories. For an ideal two-dimensional gas of spin-less particles only perpendicular magnetic field $B_\perp$ destroys the interference resulting in negative magnetoresistance, whereas an in-plane magnetic field $B_\parallel$ does not effect the interference correction.[1] Therefore, applying an in-plane magnetic field should not change the magnetoresistance caused by the perpendicular field.

For real 2D systems the situation looks more complicated and interesting. A comprehensive analysis of various aspects of magnetoresistance in 2D systems subject to an in-plane magnetic field is given in Ref. 2. Among all the mechanisms resulting in longitudinal magnetoresistance, a roughness of interface(-s) confining the 2D gas is most important for systems with one subband occupied and for considerably dirty systems in which the spin-relaxation rate is less than the dephasing rate.

Roughness of interfaces leads to an electron effectively feeling random perpendicular magnetic field at motion. This effect not only gives rise to the negative longitudinal magnetoresistance but leads to the impact of applying a fixed in-plane magnetic field upon the transverse magnetoresistance. Although the effects are small they are interesting because they give information on interface roughness of 2D structures. A detailed experimental study of effects of in-plane magnetic field on the negative magnetoresistance at perpendicular field was carried out in Ref. 4 for silicon metal-oxide-semiconductor field-effect transistor (MOSFETs). It has been found that the short-range correlated roughness ($L < l_p$, where L is the distance over which fluctuations are correlated and l_p is the mean free path) leads to a decreasing of the phase breaking time (τ_φ) with increasing in-plane magnetic field; the shape of transverse magnetoresistance curve is unaffected in this case. Theoretical analysis carried out in a recent paper by Mathur and Baranger[5] shows that the effect of an in-plane magnetic field on the shape of the transverse magnetoresistance curve strongly depends on the relationship between L, l_p, and $l_\varphi = \sqrt{D\tau_\varphi}$, where D is a diffusion coefficient. Thus, an investigation of the interference correction in the presence of an in-plane magnetic field gives a possibility to find the parameters of interface roughness in particular structure.

This paper is devoted to the experimental study of the interference induced transverse negative magnetoresistance of $GaAs/In_xGa_{1-x}As/GaAs$ quantum wells with different scales of interface roughness in the presence of strong in-plane magnetic field. It is organized as follows. In the next section we give experimental details. Experimental results presented and discussed in Sec. III, III A, and III B are dedicated to results of magnetoresistance measurements for the samples with short- and long-correlated roughness. Respectively, Sec. III C is concerned with the comparison of the results of atomic force microscopy and magnetoresistance measurements.

II. EXPERIMENTAL DETAILS

In the present work we experimentally study the two types of single quantum well heterostructures grown by

TABLE I. The parameters for the structures for different gate voltages

Structure	V_g (V)	n(10^{12} cm^{-2})	$\sigma(G_0)$[a]	σ_0 (G_0)	τ_p (10^{-13} s)	B_{tr} (T)
3512	−0.5	0.88	123.0	127.6	3.8	0.011
	−0.75	0.69	83.6	88.7	3.4	0.018
	−1.0	0.67	70.4	75.5	3.0	0.024
	−1.5	0.47	20.4	26.4	1.47	0.138
	−2.5	0.32	4.27	9.3	0.76	0.76
5610 No. 1[b]	−1.0	0.91	38.8	45.3	1.31	0.091
	−2.5	0.73	22.9	29.5	1.06	0.172
	−3.5	0.59	10.3	16.4	0.73	0.45

[a]Measured at $T=1.45$ K.

[b]The parameters of the sample 2 were close to those for sample 1.

metal-organic vapor-phase epitaxy on a semiinsulator GaAs substrate. The structure 3512 is GaAs/$In_xGa_{1-x}As$/GaAs quantum well heterostructure which consists of 0.5 μm-thick undoped GaAs epilayer, a Sn δ-layer, a 9 nm spacer of undoped GaAs, a 8 nm $In_{0.2}Ga_{0.8}As$ well, a 9 nm spacer of undoped GaAs, a Sn δ-layer, and a 300 nm cap layer of undoped GaAs. Although this structure is strained due to lattice mismatch between $In_{0.2}Ga_{0.8}As$ and GaAs, the thickness of the $In_{0.2}Ga_{0.8}As$ layer is low enough and the structure is dislocation-free.[6] In the second structure, H5610, the arrangement of the doped layers was the same as in the first one. The only difference is that the thin layer of InAs instead of $In_{0.2}Ga_{0.8}As$ layer has been grown. The large lattice mismatch between InAs and GaAs results in this case in the formation of nanoclusters. They are situated on the InAs wetting layer of one-two monolayers thickness, which serves as a quantum well for electrons. The samples were mesa etched into standard Hall bars and then an Al gate electrode was deposited by thermal evaporation onto the cap layer through a mask. Applying the gate voltage V_g we were able to change the electron density, n, and conductivity σ of 2D gas. At electron density higher than approximately 7×10^{11} cm^{-2} for structure 3512 and 9×10^{11} cm^{-2} for structure H5610, the states in δ-layers start to be occupied that affect the dephasing rate and influences the magnetoresistance curve.[7] In the present paper we restrict our consideration by the case when the states in δ-layers are empty. The structures parameters for some gate voltage are presented in Table I. The values of the Drude conductivity σ_0, the momentum relaxation time τ_p, and the so-called transport magnetic field $B_{\rm tr}=\hbar/(2el_p^2)$, have been found as described in Ref. 8. G_0 stands for $e^2/(2\pi^2\hbar)$.

In order to apply tesla-scale in-plane magnetic field while sweeping subgauss control of the perpendicular field, we mount the sample with 2D electrons aligned to the axis of primary solenoid (accurate to approximately one degree) and use an independent split-coil solenoid to provide $B_\perp$ as well as to compensate for sample misalignment. The two calibrated Hall probes were used to measure $B_\perp$ and $B_\parallel$.

III. RESULTS AND DISCUSSION

To make evident the difference in the effect of in-plane magnetic field on the shape of negative magnetoresistance at perpendicular field for structures 3512 and H5610 we have presented the data for both structures together in Fig. 1. The magnetic field scale has been normalized to $B_{\rm tr}$. One can see that the in-plane magnetic field changes the shape of the magnetoresistance curve within wide range of perpendicular field for structure 3512. For a structure H5610, the changes of the magnetoresistance shape occur mainly at the low perpendicular field, $B_\perp<0.2B_{\rm tr}$. For $B_\perp>0.2B_{\rm tr}$, the parallel magnetic field does not change the magnetoresistance curvature, it simply shifts the magnetoresistance curve up. Below we demonstrate that this difference results from the significant difference in roughness scales for these structures.

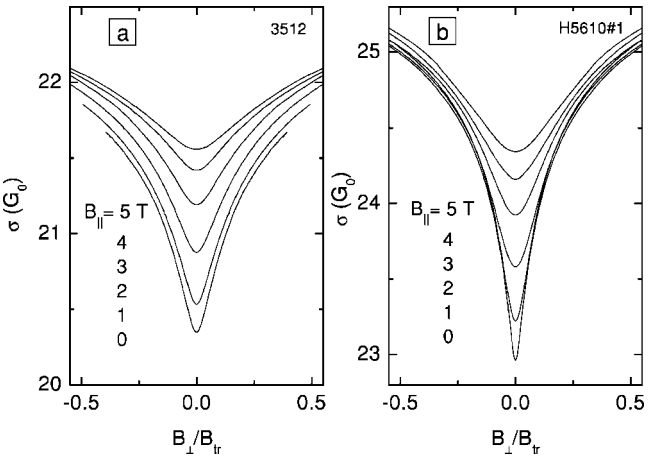

FIG. 1. The conductivity σ as a function of $B_\perp$ measured at $T=1.45$ K for different in-plane magnetic fields for structure 3512, $V_g=-1.5$ V (a) and structure H5610 No. 1, $V_g=-2.5$ V (b).

A. Role of short-range correlated roughness

Let us first consider the data for the structure 3512. Thorough studying of the weak localization correction at $B_\parallel=0$ shows that these data are in excellent agreement with conventional theory. First of all, the transverse magnetoconductance $\Delta\sigma(B)=\rho_{xx}^{-1}(B)-\rho_{xx}^{-1}(0)$ is well described by the Hikami-Larkin-Nagaoka (HLN) expression[9]

$$\Delta\sigma(B)=\alpha G_0 H(B,\tau_\varphi), \tag{1a}$$

$$H(B,\tau_\varphi)=\psi\left(\frac{1}{2}+\frac{\tau_p}{\tau_\varphi}\frac{B_{\rm tr}}{B}\right)-\psi\left(\frac{1}{2}+\frac{B_{\rm tr}}{B}\right)-\ln\left(\frac{\tau_p}{\tau_\varphi}\right), \tag{1b}$$

with α and τ_φ as fitting parameters. In Eq. (1), $\psi(x)$ is a digamma function. For a strictly diffusion regime ($\tau_p/\tau_\varphi\ll1$, $B/B_{tr}\ll1$) the prefactor α has to be equal to unity. As Fig. 2(a) illustrates, the values of the fitting parameters α and τ_φ only slightly depend on the magnetic field interval in which the fit is done, and α is close to unity that accords to low τ_p to τ_φ ratio. Second, the temperature dependence of τ_φ is close to T^{-1}-law [see Fig. 2(b)]. Finally, the temperature dependence of the conductivity at $B=0$ is logarithmic. The slope of the experimental σ/G_0-versus-ln T dependence is 1.45 ± 0.05. This slope value is determined mainly by quan-

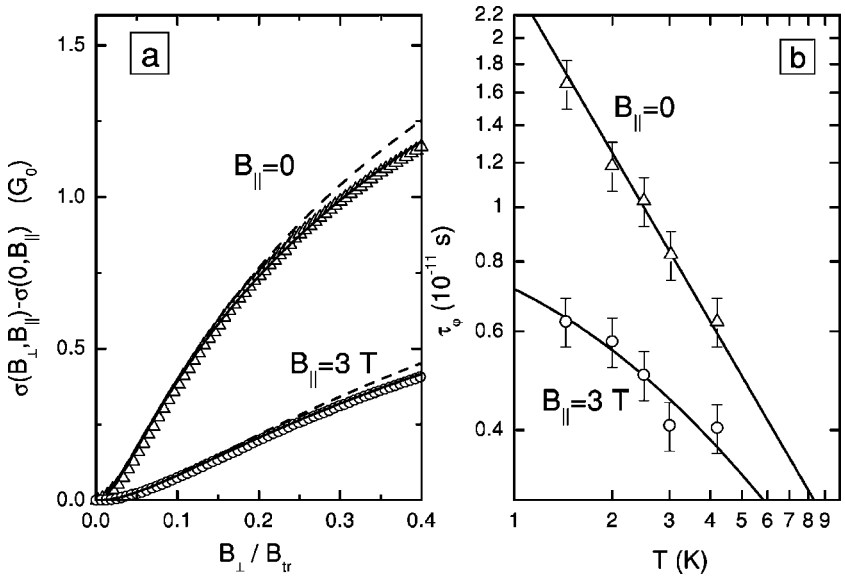

FIG. 2. (a) The $[\sigma(B_\perp,B_\parallel)-\sigma(0,B_\parallel)]$-versus-$B_\perp$ dependences for structure 3512 at $B_\parallel=0$ and 3 T, $T=1.45$ K, $V_g=-1$ V. Symbols are the experimental data. Curves are the best fit by Eq. (1) with the following parameters. For $B_\parallel=0$ they are $\alpha=0.98$ and $\tau_\varphi=1.5\times10^{-11}$ s (dashed curve), $\alpha=0.87$ and $\tau_\varphi=1.65\times10^{-11}$ s (solid curve). For $B_\parallel=3$ T the fitting parameter are $\alpha=0.75$ and $\tau_\varphi^\star=0.56\times10^{-11}$ s (dashed curve), $\alpha=0.62$, and $\tau_\varphi^\star=0.63\times10^{-11}$ s (solid curve). Dashed and solid curves correspond to the fitting interval $B_\perp=(0-0.1)B_{tr}$ and $B_\perp=(0-0.2)B_{tr}$, respectively. (b) The temperature dependence of the dephasing time for $B_\parallel=0$ and 3 T for structure 3512. Symbols are the experimental data. Upper line is T^{-1}-law, lower one is drawn as described in the text.

tum interference which contributes about 1, and the rest comes from electron-electron interaction. It should be noted that hereafter we neglect the spin-dependent effects because the spin-relaxation time is larger than the value of τ_φ under our experimental conditions.[10]

Now let us analyze the data when the in-plane magnetic field is applied. As seen from Fig. 2(a) in this case the magnetoconductance $\sigma(B_\perp,B_\parallel)-\sigma(0,B_\parallel)$ is well described by Eq. (1) also and the fitting parameters α and $\tau_\varphi^\star$ (hereinafter, τ_φ relating to $B_\parallel\neq0$ will be labelled as $\tau_\varphi^\star$) depend only slightly on the fitting interval. The prefactor value noticeably decreases with $B_\parallel$ increase. The behavior of $\tau_\varphi^\star$ with $B_\parallel$ is illustrated by Fig. 3(a). As clearly seen, the value of $\tau_\varphi^\star$ strongly decreases when $B_\parallel$ increases.

The effect of the in-plane magnetic field on the transverse negative magnetoresistance can be understood as follows. The weak localization correction to the conductivity results from the interference of electron waves scattered along closed trajectories in opposite directions (time-reversed paths). A magnetic field gives the phase difference between time-reversed paths and thus destroys the interference and results in the negative magnetoresistance. Ideal 2D systems do not feel an in-plane magnetic field at all because the path within the plane enclose no flux of $B_\parallel$. In real 2D structure the mean electron position in growth direction randomly changes at motion along closed paths due to interface roughness. Therefore, an in-plane magnetic field leads to an additional dephasing and, thus, influences the magnetoresistance measured at $B_\perp$. Theoretical analysis[4,5,12] shows that for the case of short-range correlated roughness the role of in-plane magnetic field reduces to increasing of the dephasing rate

$$\frac{1}{\tau_\varphi^\star}=\frac{1}{\tau_\varphi}+\frac{1}{\tau_\parallel}, \tag{2}$$

where $\tau_\parallel^{-1}$ is determined by parameters of roughness[5]

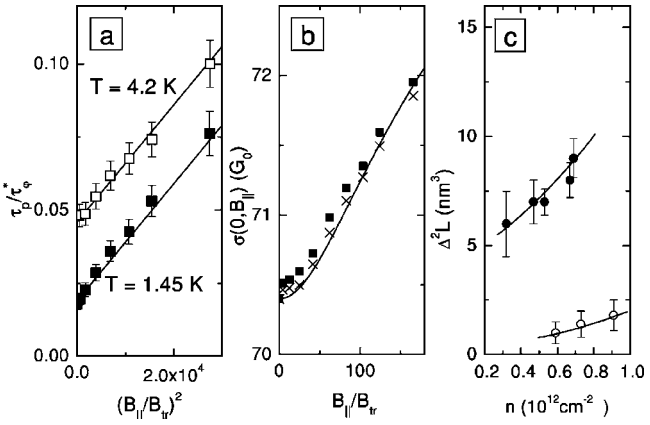

FIG. 3. (a) The value of $\tau_p/\tau_\varphi^\star$ as a function of $B_\parallel^2$ for structure 3512 at $T=1.45$ and 4.2 K, $V_g=-1$ V. Symbols are experimental results. Lines are calculated from Eqs. (2) and (3) using $\Delta^2L=7.2$ nm^3, $l_p=117$ nm, $\tau_p/\tau_\varphi=0.018$ ($T=1.45$ K), and 0.048 ($T=4.2$ K). (b) The conductivity as a function of in-plane magnetic field for structure 3512, $T=1.45$, $V_g=-1$ V. Squares are the experimental results. Crosses are calculated as $\sigma(B_\parallel)=\sigma(B_\parallel=0)+\ln(\tau_\varphi/\tau_\varphi^\star)$, where τ_φ and $\tau_\varphi^\star$ have been obtained from the fit of experimental curve $\Delta\sigma(B_\perp)$ at $B_\parallel=0$ and $B_\parallel\neq0$, respectively. Solid line is Eq. (4b) with $\Delta^2L=7.2$ nm^3 and $l_p=117$ nm. (c) The electron density dependence of the parameter Δ^2L for structures 3512 (solid symbols) and H5610 (open symbols). Lines are provided as a guide to the eye.

$$\frac{1}{\tau_{\|}} \simeq \frac{1}{\tau_p}\frac{\sqrt{\pi}}{4}\frac{\Delta^2 L}{l_p^3}\left(\frac{B_{\|}}{B_{\rm tr}}\right)^2. \tag{3}$$

Here, Δ is the root-mean-square height of the fluctuations, and L is the distance over which the fluctuations are correlated.

Let us consider how our experimental results for structure 3512 agree with this model. Figure 3(a) shows that $\tau_p/\tau_\varphi^\star$ increases linearly with $B_{\|}^2$ in full agreement with Eqs. (2) and (3), therewith the slope of this dependence is temperature independent. In the framework of this model the temperature dependence of $\tau_\varphi^\star$ in the presence of an in-plane magnetic field has to converge toward $\tau_{\|}$ with decreasing temperature. Figure 2(b) in which the experimental results obtained for $B_{\|}=3$ T are plotted shows that $\tau_\varphi^\star$-versus-T dependence really tends to saturate at $T\to 0$. In the same figure we plot the $\tau_\varphi^\star$-versus-T curve calculated in accordance with Eq. (2). In this calculation the dependence $2.5\times 10^{-11}/T$ which is a good interpolation of experimental data for $B_{\|}=0$ [see Fig. 2(b)] has been used as $\tau_\varphi(T)$ in the right-hand side of Eq. (2). The quantity $\tau_{\|}^{-1}=1\times 10^{11}$ s^{-1} has been obtained as a difference between two values $(\tau_\varphi^\star)^{-1}$ and τ_φ^{-1} found experimentally at $T=1.45$ K. Good agreement is evident within the whole temperature range.

This model predicts also that the growth of the in-plane magnetic field has to lead to an increase of conductivity at $B_\perp=0$

$$\sigma(0,B_{\|}) = \sigma(0,0) + G_0 \ln\frac{\tau_\varphi}{\tau_\varphi^\star} \tag{4a}$$

$$\simeq \sigma(0,0) + G_0 \ln\left[1 + \frac{\tau_\varphi}{\tau_p}\frac{\sqrt{\pi}}{4}\frac{\Delta^2 L}{l_p^3}\left(\frac{B_{\|}}{B_{\rm tr}}\right)^2\right]. \tag{4b}$$

In Fig. 3(b) we present the in-plane magnetic field dependence of the conductivity which was measured and was calculated from Eq. (4a) using $\tau_\varphi^\star$ found above [see Fig. 3(a)]. One can see that within experimental error these data agree with each other satisfactorily. Finally, the decrease of prefactor α with growing $B_{\|}$ is also transparent in framework of this model. The parallel magnetic field strongly increases the dephasing rate and violates one of the conditions of diffusion regime: $\tau_p \ll \tau_\varphi$. For instance, $\tau_p/\tau_\varphi^\star \simeq 0.075$ for $B_{\|}=4$ T, $T=1.45$ K [see Fig. 3(a)], which is clearly not enough for the diffusion approximation.[13] In this case, strictly speaking, the Eq. (1) is not valid anymore. Nevertheless, as shown in Ref. 13 the use of Eq. (1) for the fit of experimental data beyond the diffusion regime gives the value of the phase relaxation time very close to the true one and the prefactor value less than unity.

Thus, all effects predicted for the case of the short-range correlated roughness are observed in the structure 3512. Therefore we believe that the slope of $\tau_p/\tau_\varphi^\star$-versus-$(B/B_{\rm tr})^2$ dependence gives the parameter of roughness $\Delta^2 L$. With the use of the data from Fig. 3(a) we estimate the parameter of roughness $\Delta^2 L$ as 7.2 nm^3 for $V_g=-1$ V. Naturally, Eq. (4b) with this value of $\Delta^2 L$ well describes the experimental in-plane magnetic field dependences of the conductivity, measured without perpendicular magnetic field [Fig. 3(b)].

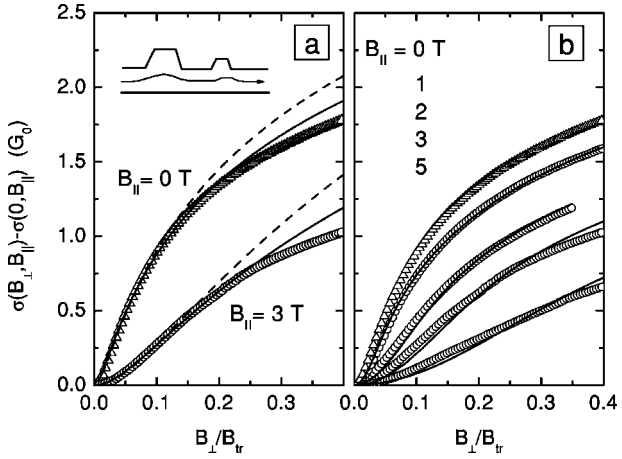

FIG. 4. The $[\sigma(B_\perp,B_{\|})-\sigma(0,B_{\|})]$-versus-$B_\perp$ dependences for structure H5610 No. 2 taken at $T=1.45$ K and $V_g=-2.5$ V. Symbols are the experimental data. Curves in (a) are the best fit by Eq. (1) with parameters: $B_{\|}=0-\alpha=1.0$, $\tau_\varphi=1.2\times 10^{-11}$ s (dashed line) and $\alpha=0.9$, $\tau_\varphi=1.45\times 10^{-11}$ s (solid line); $B_{\|}=3$ T$-\alpha=2.2$, $\tau_\varphi=2.3\times 10^{-12}$ s (dashed line) and $\alpha=1.4$, $\tau_\varphi=2.9\times 10^{-12}$ s (solid line). Dashed and solid curves correspond to the fitting interval $B_\perp=(0-0.1)B_{tr}$ and $B_\perp=(0-0.2)B_{tr}$, respectively. Curves in (b) are the best fit by Eq. (5) in which the Gaussian distribution and experimental curve $\sigma(B_\perp,0)$ are used for $F(\beta)$ and $\delta\sigma(B_\perp+\beta B_{\|},\tau_\varphi)$, respectively. The values of fitting parameter Δ_β for $B_{\|}$ from $B_{\|}=1$ T to $B_{\|}=5$ T are the following: 0.34°; 0.41°; 0.47°; 0.52°. Inset in (a) is a schematic representation of electron motion along the quantum well with one rough interface.

We have carried out such analysis for various gate voltages and plotted the electron density dependence of $\Delta^2 L$ in Fig. 3(c). One can see that the value of $\Delta^2 L$ somewhat decreases with decreasing electron density. This observation can be understood if we assume that the outer interface bordering the quantum well is more rough than the back interface. With the decrease of the gate voltage, i.e., with a decrease of the electron density, the wave function moves away from the outer rough interface that reduces its role in the weak localization. The larger roughness of the outer interface is natural for the GaAs/In$_x$Ga$_{1-x}$As/GaAs quantum well heterostructures.[14] Analogous results were obtained in Ref. 4 for silicon MOSFET.

B. Effect of nanoclusters on the weak localization

Now we are in position to consider the effect of in-plane magnetic field on the transverse magnetoresistance for structure H5610 with nanoclusters. The $[\sigma(B_\perp,B_{\|})-\sigma(0,B_{\|})]$-versus-$B_\perp$ plots for structure H5610#2 are presented in Fig. 4. As seen from Fig. 4(a) the negative magnetoresistance measured at $B_{\|}=0$ is well described by Eq. (1). If one tries to fit the data measured at $B_{\|}\neq 0$ by Eq. (1) one finds that the fitting parameters depend on the fitting interval strongly in contrast to the structure 3512. To illustrate, the prefactor α strongly decreases from $\alpha=2.2$ to $\alpha=1.4$ when the fitting interval of $B_\perp$ is expanded from $(0-0.1)B_{\rm tr}$ to $(0-0.2)B_{\rm tr}$ [see Fig. 4(a)]. What this means is the HLN-expression (1) describes the experimental data for

structure H5610 inadequately. Even if it is granted that the HLN-formula is applicable in this case, the prefactor demonstrates the behavior which is opposite that for structure 3512. The value of α increases with increasing $B_\parallel$, whereas it decreases in structure 3512 due to an increase of τ_p to τ_φ ratio. Finally, the significantly higher than unity value of the prefactor seems to be unreasonable. To our knowledge, a valley degeneracy or existence of several subbands occupied results in $\alpha > 1$. Apparently, it is not our case. We believe that all these peculiarities originate from the presence of long-range correlated roughness in structure H5610 which is caused by nanoclusters. The presence of nanoclusters leads to the fact that the electron motion is not two dimensional anymore, the mean electron position fluctuates now in the structure growth direction during the motion along the quantum well, as is shown in inset in Fig. 4(a).

Influence of an in-plane magnetic field on the shape of magnetoresistance curve in perpendicular field for the case $L > l_p$ was theoretically studied in Ref. 5. However the final expressions are very complicated and cumbersome to compare with the experimental curves directly. Another limiting case $L > l_\varphi$ is very simple and transparent from the physical point of view. In this case one can consider that all the actual closed paths lie on the flat elements of size larger than l_φ, which are inclined from an ideal 2D plane through small random angles β. This means that the resulting magnetoresistance is a sum of the contributions of these deflected elements. The contribution of each element is $\delta\sigma(B_n, \tau_\varphi) \simeq \delta\sigma(B_\perp + \beta B_\parallel, \tau_\varphi)$, where B_n is the projection of the total magnetic field onto the normal to the element plane. Then, the total magnetic field dependence of the conductivity can be written as

$$\sigma(B_\perp, B_\parallel, \tau_\varphi) = \int d\beta F(\beta)\, \delta\sigma(B_\perp + \beta B_\parallel, \tau_\varphi), \qquad (5)$$

where $F(\beta)$ is the distribution function of the deflection angles. Note, this expression works at any relationship between $B_\perp$ and $\beta B_\parallel$ and, in this sense, is more general than Eq. (83) from Ref. 5, which has been obtained for $\beta B_\parallel \ll B_\perp$. To compare Eq. (5) with experimental data one needs to specify the functions in the right-hand side of Eq. (5). We have used the Gaussian distribution for $F(\beta)$ with root-mean-square Δ_β. The experimental σ-versus-$B_\perp$ curve measured at $B_\parallel = 0$ has been used as $\delta\sigma(B_\perp + \beta B_\parallel, \tau_\varphi)$. An advantage of such an approach in comparison with the use of equations (76)–(78) from Ref. 5 is the existence of only a single fitting parameter Δ_β. The result of the fitting procedure for $\sigma(B_\perp, B_\parallel) - \sigma(0, B_\parallel)$ is shown in Fig. 4(b). One can see that this simple model perfectly describes the shape of the experimental magnetoresistance curve in the presence of the in-plane magnetic field up to $B_\parallel = 2$ T, the parameter Δ_β found from the fit is really small in magnitude: $\Delta_\beta \simeq 0.3° - 0.4°$.

A noticeable discrepancy between this simple model and experimental observations is evident in the shape of the magnetoconductance curve in high parallel magnetic field, $B_\parallel \gtrsim 3$ T. Moreover, the parameter Δ_β sufficiently increases with $B_\parallel$ increase [see Fig. 5(a)] that seems unnatural. The situation can be improved if one supposes a simultaneous

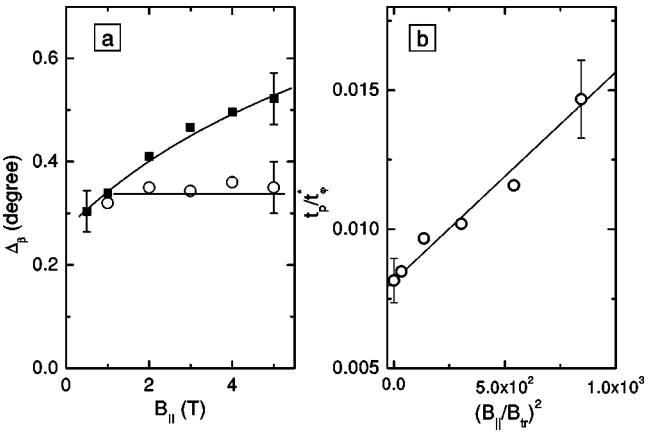

FIG. 5. The fitting parameters Δ_β (a) and $\Delta^2 L$ (b) corresponding to solid lines in Fig. 6(b) as functions of in-plane magnetic field. Solid symbols correspond to the long-range roughness model, open symbols are obtained when both short- and long-range roughness are taken into consideration. Lines in (a) are provided as a guide to the eye, line in (b) is calculated from Eqs. (2) and (3) using $\Delta^2 L = 1.4$ nm^3 and experimental values $l_p = 44$ nm and $\tau_p/\tau_\varphi = 8.15 \times 10^{-3}$.

existence of short- and long-range correlated roughness in structure H5610. As shown above the short-range correlated roughness results effectively in lowering of τ_φ in in-plane magnetic field. Thus, it becomes meaningless to use the experimental σ-versus-$B_\perp$ curve measured at $B_\parallel = 0$ in the right-hand side of Eq. (5) when $B_\parallel$ is rather high.

The presence of short-range correlated roughness in structure H5610 is more pronounced when considering the effect of an in-plane magnetic field on the absolute value of the conductivity. Figure 6(a) shows the same calculated curves as in Fig. 4(b) but plotted without subtraction of $\sigma(0, B_\parallel)$. Comparing this figure with Fig. 6(b), in which the experi-

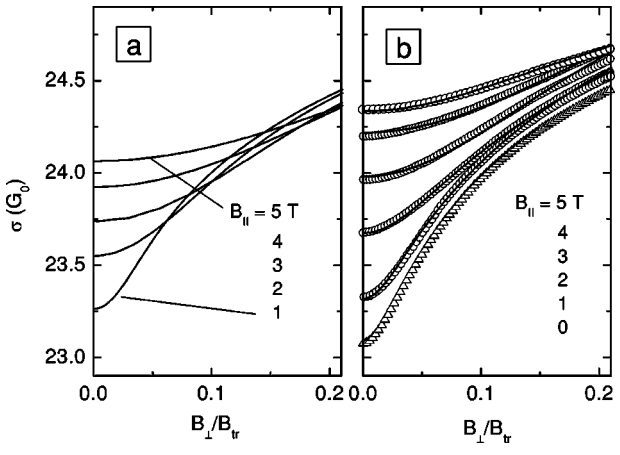

FIG. 6. The $B_\perp$-dependences of absolute values of the conductivity taken at different in-plane magnetic field. Lines in (a) are just the same as in Fig. 4(b) but plotted without subtraction of the value of $\sigma(0, B_\parallel)$. Symbols in (b) are the experimental data for structure H5610 No. 2 obtained at $T = 1.45$ K and $V_g = -2.5$ V, lines are obtained taking into account both long- and short-range correlated roughness. The fitting parameters as a function of in-plane magnetic field are shown in Fig. 5.

mental results are presented, one can see that the model taking into consideration only the long-range correlated roughness does not describe the behavior of absolute value of σ in the in-plane magnetic field. It is most conspicuous at $B_\perp/B_{tr} \gtrsim 0.1$, where the experimental σ-versus-$B_\perp$ plots are shifted up with a $B_\parallel$-increase whereas the calculated curves tend to merge together. It is natural to suggest that the shift of experimental curves is a result of the influence of short-range correlated roughness which leads to a decrease of τ_φ and, thus, to an increase of the conductivity with increasing of an in-plane magnetic field when the perpendicular field is fixed.

To take into account the coexistence of both long- and short-range correlated roughness in our model, we have used the quantity $\sigma(B_\perp=0, B_\parallel=0)+\Delta\sigma(B,\tau_\varphi)$ as $\delta\sigma(B_\perp+\beta B_\parallel, \tau_\varphi)$ in Eq. (5), where $\sigma(B_\perp=0, B_\parallel=0)$ is measured experimentally and $\Delta\sigma(B,\tau_\varphi)$ is given by Eq. (1). So, manipulating by three fitting parameters α, τ_φ, and Δ_β we, naturally, achieve an excellent agreement between experimental results and the model taking into account both types of roughness [see Fig. 6(b)].

Let us now consider whether the fitting parameters are reasonable. First, the value of the prefactor is about 0.8–0.9 that agrees with sufficiently large τ_φ to τ ratio at any $B_\parallel$: $\tau_\varphi^\star/\tau \simeq 60-120$. Second, as seen from Fig. 5(a) the parameter Δ_β now behaves appropriately: it is practically independent of $B_\parallel$ and, what is important, its value is close to that obtained above without taking into account the short-range correlated roughness. The latter indicates once again that the influence of low $B_\parallel$ on the weak localization is mainly due to the long-range correlated roughness. Thus, the value of Δ_β characterizing the long-range correlated roughness can be estimated as 0.35°. Finally, the fitting parameter $1/\tau_\varphi^\star$ exhibits quadratical increase when $B_\parallel$ increases [see Fig. 5(b)], that allows us to estimate the scale of the short-range correlated roughness using Eqs. (2) and (3). The value of $\Delta^2 L$ in structure H5610 with nanoclusters occurs to be about 1.4 nm^3 at $V_g=-2.5$ V, which is less than that for structure 3512. Such an analysis carried out for other gate voltages shows that the parameter Δ_β is independent of the electron density within experimental error and, thus, is about 0.35° and the parameter $\Delta^2 L$ increases from approximately 1 to 1.8 nm^3 when the electron density varies from 0.59×10^{12} to 0.91×10^{12} cm^{-2} [see Fig. 3(c)]. As well as for structure 3512 (see Sec. III A), we believe that such a behavior of $\Delta^2 L$ is a result of the shift of the wave function to an inner smooth interface of the quantum well that in its turn leads to the reduction of the role of outer rough interface.

Thus, for the 2D structure with nanoclusters we can adequately describe the influence of the in-plane magnetic field on weak localization combining two limiting theoretical models corresponding to short- and long-range correlated roughness.

C. Results of atomic force microscope studies

To assure that the structure H5610 distinguishes from structure 3512 by the presence of long-range correlated roughness and to estimate its parameters, we have attempted

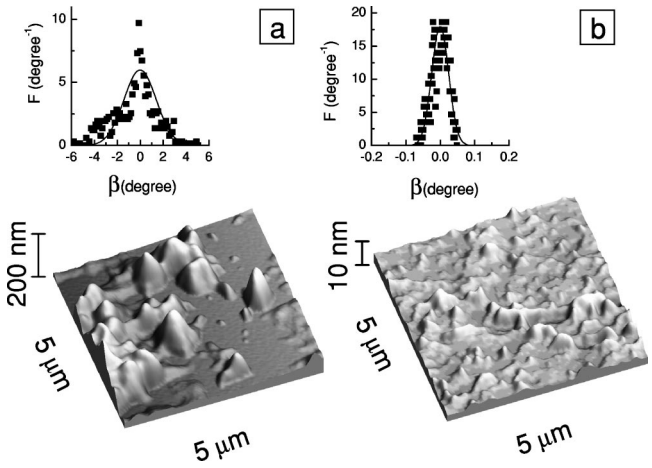

FIG. 7. The AFM images for structure H5610 (a) and 3512 (b) obtained after removing of the cap layer. Insets show the angle distribution function $F(\beta)$ obtainedfor $\mathcal{L}=2l_\varphi$ (see text). The values of l_φ at $T=1.5$ K are 490 nm and 870 nm for structures H5610 and 3512, respectively.

to measure the profile of the quantum well surface. For this purpose the cap layer was removed using the selective etching.[15–17] After that the surface was scanned by atomic force microscope (AFM) using TopoMetrix Accurex TMX-2100 ambient air AFM in Contact Mode. Si_3N_4 pyramidal probes were employed. The AFM images for both structures are shown in Fig. 7. It is clearly seen that the scales of surface roughness are drastically different. The main difference is that the amplitude of the roughness of lateral size $\mathcal{L} > l_\varphi$ (the values of l_φ found at $T=1.5$ K are 870 and 490 nm for structures 3512 and H5610, respectively) is significantly larger for structure H5610. In order to get the quantitative information corresponding to our weak-localization experiments, we have processed the images.

Let us consider the long-range roughness. First of all, the correlation analysis of AFM images for structure H5610 shows that the correlation length, $L \simeq 1$ μm, is really greater than the dephasing length, $l_\varphi \simeq (300-500)$ nm for different gate voltages, $T=1.5$ K. This fact justifies the model used in Sec. III B for analysis of the transverse negative magnetoresistance in the presence of an in-plane magnetic field for structure H5610. Furthermore, in accord with this model the scan surface was approximated by a set of the flat squares of size $\mathcal{L} > l_\varphi$, then the angle distribution function $F(\beta)$ entering in Eq. (5) was found. The result is presented in the inset of Fig. 7(a). We have approximated the angle distribution data by the Gaussian distribution and found the dispersion Δ_β. The values of Δ_β obtained for $\mathcal{L}=2l_\varphi$ and $\mathcal{L}=3l_\varphi$ are close with an accuracy of about 30%. As seen from the inset the value of Δ_β is about 2° that is approximately six times larger than the dispersion obtained from the weak localization measurements [see Fig. 5]. The reason for such a discrepancy is qualitatively clear. In reality, an electron moves not over the surface, it moves in the quantum well laying under the surface. Therefore, the deviations of an electron in the z-direction are smaller than the magnitude of surface roughness. Thus, we consider the results of weak localization and AFM experiments being in a satisfactory agreement for structure H5610.

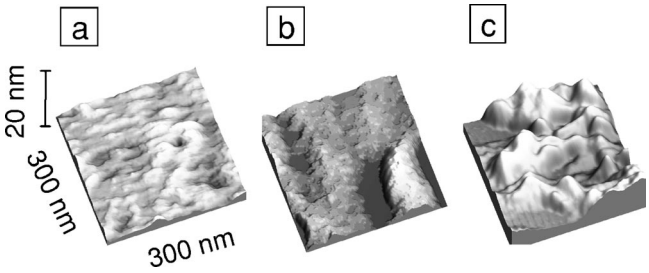

FIG. 8. The AFM images for structure 3512 (a) and H5610 for flat (b) and hilly (c) areas.

Such a scan processing made for structure 3512 gives the dispersion Δ_β about 0.035° [see inset in Fig. 7(b)], i.e., the long-range correlated roughness is practically absent. This fact agrees with the experimental result that only the short-range correlated roughness reveals itself in weak localization in the presence of in-plane magnetic field.

To estimate the parameter $\Delta^2 L$ responsible for the influence of the short-range correlations on the weak localization, the surfaces have been scanned with the higher resolution (Fig. 8). The mean peak spacing for structure 3512 found from AFM-image given in Fig. 8(a) is 65 nm, that is really less than the mean free path ($l_p = 210$ nm for $V_g = 0$). Therefore, the use of the short-range correlated roughness model is justified. The value of Δ found as a root-mean-square deviation in the z-direction is about 0.35 nm. So, we obtain from the independent AFM measurements the parameter $\Delta^2 L \simeq 8$ nm^3 which is close to that obtained from the weak-localization experiment [see Fig. 3(c)].

It is more difficult to carry out the analogous estimation for structure H5610. First, the flat and hilly areas look differently at this resolution [see Figs. 8(b) and 8(c)]. Second, the peak spacing distribution is very wide and has no maximum. Nevertheless, we try to estimate the parameter $\Delta^2 L$ relevant for the contribution of the short-range correlated roughness to the weak localization assuming that all the roughnesses with lateral size less than $l_p/2$ are actual. Then, the parameter Δ can be estimated as the mean-root-square deviation in the z-direction, which is found on the length $l_p/2$ and averaged over the surface. The value of Δ found for the flat and hilly areas appears to be different: 0.2 and 0.6 nm, respectively. Therefore, the values of parameter $\Delta^2 L = \Delta^2 l_p/2$ differ significantly for these areas: 1.6 and 14 nm^3 (we use here $l_p = 80$ nm that corresponds to $V_g = 0$). Recall that $\Delta^2 L$ obtained from the weak localization experiments is (1.5–2.5) nm^3 [see Fig. 3(c)]. Taking into account the large scatter of AFM results, we consider such an agreement satisfactory.

IV. CONCLUSION

We have experimentally studied the effects of an in-plane magnetic field on the interference induced negative magnetoresistance in perpendicular magnetic field for different types of quantum well heterostructures. It has been shown that the effects significantly depend on the relationship between the mean-free-path and an in-plane size of the roughness. The analysis of the shape of the negative magnetoresistance at an in-plane magnetic field allows us to recognize the characteristic in-plane scale of the roughness and estimate its parameters. The results of weak localization studies have been found in a good agreement with evidence from AFM measurements.

ACKNOWLEDGMENTS

This work was supported in part by the RFBR through Grant Nos. 01-02-16441, 03-02-16150, 03-02-06025, and 04-02-16626, the CRDF through Grant Nos. EK-005-X1 and Y1-P-05-11, and the Russian Program *Physics of Solid State Nanostructures*.

*Electronic address: grigori.minkov@usu.ru

[1] Julia S. Meyer, Alexander Altland, and B. L. Altshuler, Phys. Rev. Lett. **89**, 206601 (2002).

[2] Julia S. Meyer, Vladimir I. Fal'ko, and B. L. Altshuler, in NATO Science Series II, Vol. 72, edited by I. V. Lerner, B. L. Altshuler, V. I. Fal'ko, and T. Giamarchi (Kluwer Academic, Dordrecht, 2002), pp. 117–164.

[3] A. G. Malshukov, K. A. Chao, and M. Willander, Phys. Rev. B **56**, 6436 (1997).

[4] P. M. Mensz and R. G. Wheeler, Phys. Rev. B **35**, 2844 (1987).

[5] H. Mathur and Harold U. Baranger, Phys. Rev. B **64**, 235325 (2001).

[6] E. P. O'Reilly, Semicond. Sci. Technol. **4**, 121 (1989).

[7] G. M. Minkov, A. V. Germanenko, O. E. Rut, A. A. Sherstobitov, B. N. Zvonkov, E. A. Uskova, and A. A. Birukov, Phys. Rev. B **64**, 193309 (2001).

[8] G. M. Minkov, O. E. Rut, A. V. Germanenko, A. A. Sherstobitov, B. N. Zvonkov, E. A. Uskova, and A. A. Birukov, Phys. Rev. B **65**, 235322 (2002).

[9] S. Hikami, A. Larkin, and Y. Nagaoka, Prog. Theor. Phys. **63**, 707 (1980).

[10] The study of the electron energy spectrum and weak localization, carried out in Ref. 11 for the samples investigated, shows that the main contribution to the spin splitting comes from the Dresselhaus mechanism and its maximal value, $\hbar\Omega \simeq 0.1$ meV, is achieved for $n = 10^{12}$ cm^{-2}. If one supposes that the Dyakonov–Perel mechanism determines the spin relaxation and uses the maximal value 4×10^{-13} s for τ_p (see Table I), we obtain the lower estimate for the spin relaxation time, τ_s, in our case: $\tau_s = 1/(2\Omega^2 \tau_p) \simeq 5 \times 10^{-11}$ s. This value is several times larger than the maximal value of τ_φ [see Fig. 2(b)] and, therefore, the spin dependent effects can be ignored. Since applying an in-plane magnetic field decreases τ_φ due to interface roughness and increases τ_s (Refs. 3 and 12) this approximation is justified at $B_\parallel \neq 0$ as well.

[11] G. M. Minkov, A. V. Germanenko, O. E. Rut, A. A. Sherstobitov, and B. N. Zvonkov, Int. J. Nanosci. **2**, 543 (2003).

[12] A. G. Malshukov, V. A. Froltsov, and K. A. Chao, Phys. Rev. B

59, 5702 (1999).
[13] G. M. Minkov, A. V. Germanenko, V. A. Larionova, S. A. Negashev, and I. V. Gornyi, Phys. Rev. B **61**, 13164 (2000).
[14] Kuo-Jen Chao, Ning Liu, Chih-Kang Shih, D. W. Gotthold, and B. G. Streetman, Appl. Phys. Lett. **75**, 1703 (1999).
[15] R. Retting and W. Stolz, Physica E (Amsterdam) **2**, 277 (1998).
[16] I. A. Karpovich, N. V. Baidus, B. N. Zvonkov, D. O. Filatov, S. B. Levichev, A. V. Zdoroveishev, and V. A. Perevoshikov, Phys. Low-Dimens. Semicond. Struct. **3/4**, 341 (2001).
[17] I. A. Karpovich, A. V. Zdoroveichev, A. P. Gorshkov, D. O. Filatov, and R. N. Skvortsov, Phys. Low-Dimens. Semicond. Struct. **3/4**, 191 (2003).